Effect of Solidus Temperature and Crystalline Phase of Mold Flux on Heat Transfer in Continuous Casting Mold

Akira Yamauchi[1], Kenichi Sorimachi[2] and Takashi Yamauchi[3]

[1] Technical Research Laboratories, Kawasaki Steel Corporation,
Kawasaki-cho 1, Chuo-ku, Chiba, 260-0815, Japan
(Presently a doctor student at the Division of Metallurgy,
Division of Metallurgy, Department of Material Science and Engineering,
Royal Institute of Technology
Brinellvagen 23, SE-100 44 Stockholm, Sweden
FAX: +46 –8 790 0939, PHONE: +46 –8 790 9568)

[2] Research Laboratories, Kawasaki Refractories Co., LTD
1576-2 Aza-Higashioki, Nakahiro, Akoh, Hyogo, 678-0232, Japan

[3] Chiba Works, Kawasaki Steel Corporation,
Kawasaki-cho 1, Chuo-ku, Chiba, 260-0815, Japan.

Keyword: mold flux, heat transfer, thermal conductivity, conduction, radiation, contact resistance, crystallization, solidus, continuous casting,

Abstract:

Pieces of mold flux film obtained from commercial continuous casting machine and measurements of the mold temperature were investigated to explain the mechanism of heat transfer in the mold. Comparing to the results of numerical calculation, the main factor to determine the reduction of heat transfer with high basicity flux is contact resistance at the interface of the mold wall and solid flux film. The results show that relatively high contact resistance is introduced with crystalline and high-solidus mold flux because of the stability of contact resistance.

INTRODUCTION

Heat transfer though mold flux layer in continuous casting mold is very important factor to determine slab surface quality such as cracks and oscillation marks. One of the most effective measures to prevent cracks is to use basic mold flux with higher crystallising temperature [1]. The crystalline phase in solid flux film produces larger thermal resistance at the interface of flux and mold wall [2]. The thermal resistance reduces unevenness of the heat transfer in the mold. Though there have been reported various evidences such as the relationship between heat transfer and conduction [3,4], radiation and formation of air gap on crystalline phase of mold flux film, the mechanism of the heat flux reduction have not been cleared enough yet.

The objective of present study is to clarify main factors to determine the heat transfer through flux film at meniscus region in the mold with measurement of physical properties of mold flux, observation of flux films taken from continuous casting experiments and numerical simulation.

REDUCTION OF HEAT FLUX WITH HIGH BASICITY MOLD FLUX

Figure 1 shows the reduction of local heat flux in a continuous casting mold with high basicity mold flux. About 15% of reduction are observed in this case. Many reports [1-4 for example] have explained the reduction and improvement of cracking on slab surface with high basicity mold flux. The mechanisms are categorised as follows:

1) Effective thermal conductivity of solid phase in the flux film decreases owing to increase of micro pores with high basicity [1].
2) Radiation term in the heat transfer decreases owing to opaqueness of crystalline phase for infrared with high basicity [2].
3) Increase of contact thermal resistance at the interface of the solid flux film and the mold wall owing to increase of surface roughness that develops when crystallisation [2-4].

The thermal conductivity of the crystalline phase can be twice as large as that of liquid or glassy phase. Therefore the effective thermal conductivity does not decrease

very much when crystallised. The effect of 1) is relatively small comparing to the others. The existence of crystalline phase decreases the radiation through flux film as mentioned in 2). Cho et al. [3] and Yamauchi et al. [2] have been estimated the contribution of radiation term to the reduction of the total heat transfer by experiments and numerical simulations. However, the contribution is only 2 to 5% of total heat transfer. The effect of crystallisation on the formation of the thermal resistance has been investigated by Suzuki [4], Yamauchi [2], Shibata [5] and Tsutsumi et al. [6]. These reports have only focused on relationship between the crystallisation and the formation of surface roughness on the flux film. The value of the contact resistance may not be the same value as it was formed at the beginning with large thermal resistance since the flux film temperature at the interface cannot exceed the melting temperature (or liquidus) of film itself. This limitation suggests the relationship between actual contact resistance and solidus of used mold flux.

The numerical simulation considering the limitation is necessary to evaluate the effect of physical properties of mold flux.

NUMERICAL SIMULATION AND MEASURING PHYSICAL PROPERTIES OF FLUX

NUMERICAL SIMULATION

Heat transfer model used in the numerical simulation is shown in Figure 2 with assuming one dimensional heat transfer. Convection term is negligible small because the thickness of the liquid film is very small such as only a few hundred micrometers. (Eq. (1)) The procedures of the calculation are shown in Figure 3. Before starting the calculation, absorption coefficient of the flux and emissivity are necessary to evaluate radiation term, q_r (Eq. (2))

$$q = q_c + q_r$$
$$= (T_s - T_m)\frac{\lambda_c}{d_p} + \alpha(T_s^4 - T_m^4) \qquad (1)$$

Where

$$\alpha = \frac{n^2 \sigma}{0.75 a d_p + \varepsilon_s^{-1} + \varepsilon_m^{-1} - 1} \qquad (2)$$

STATIC SIMULATION WITH PARALLEL PLATE METHOD

In order to obtain thermal properties of mold flux, laboratory experiments have been carried out with parallel plate method [2]. Figure 4 shows a schematic representation of the experimental apparatus. Temperatures in a cooling block and AlN plate were measured in various thickness of mold flux films when steady state. Figure 5 shows an example of the result.

Assuming that the contribution of convection is negligible small, heat flux through the flux film is expressed as Eq. (1). Therefor the relationship between $\frac{q}{T_s - T_m}$ and $T_s^3 + T_s^2 T_m + T_s T_m^2 + T_m^3$ is liner as shown in Eq. (3) and □ can be derived as the slope of the plot for each d_p.

$$\frac{q}{T_s - T_m} = \alpha (T_s^3 + T_s^2 T_m + T_s T_m^2 + T_m^3) + \frac{\lambda_c}{d_p} \qquad (3)$$

λ_c is derived from the slope of the plot and given d_p.

Since the value of α is a function of d_p as expressed in Eq. (2), the relationship between d_p and $\frac{n^2 \sigma}{\alpha}$ is also liner as shown in Figure 5. Assuming constant n [7], the absorption coefficient of the flux, **a**, is the slope of the plot. The value of y-axis interception stands for $\varepsilon_s^{-1} + \varepsilon_m^{-1} - 1$. Two different types of mold flux were measured to show the extreme cases. Flux A represents low solidus and Flux B represents high solidus. The chemical compositions are shown in Table 1. Solidus and liquidus temperatures in the Table 1 were measured with laser scanning microscope (LSM, Lasertech Co.) and confirmed by DSC (Heating up rate was $5Ks^{-1}$ for both method.) Both Flux A and B tend to produce crystalline phase when they solidify

since they contain more oxides of alkali and alkali earth than SiO_2 in the chemical composition. The measurements of Flux A and B are summarised in Table 2.

HEAT TRANSFER IN ACTUAL CASTING MOLD

Evaluation of the heat transfer through the mold flux film in the mold has been carried out with pilot scale continuous caster in Technical Research Division (in Chiba Works), Kawasaki Steel Co. The steel grade used in casting was medium-carbon steel (approximately 0.11%C) which is sensitive to cracking. In each casting experiment, 5.0×10^3 kg of molten steel was cast into a slab approximately 14 m in length and the casting time is about 10 min. The temperature of the molten steel in the tundish was 1830K at casting start and 1820K at the completion of casting, and the average superheat of the molten steel was 30K. During casting, the meniscus was controlled automatically to a position 100 mm from the top edge of the mold at all times by a eddy current sensor. A total number of 34 K-type thermocouples were buried in the mold plates to measure the temperature of the mold inner wall surfaces and the local heat flux of the mold. Mold temperature measurement sampling was performed at intervals of one second.

A result of the heat flux measurement is shown in Figure 6. There are peaks of the local heat flux for each mold flux at just below meniscus in the Fig. 6 (a). The value of the peak for flux B is about 20% smaller than that for flux A.

A stainless wire gauze was set just below the mold in order to collect pieces of flux film. Thickness of the pieces and surface roughness, that are necessary for the numerical calculation, were measured. Examples of film pieces for each mold flux and LSM images for measuring surface roughness are shown in Figure 7 and 8 respectively. The roughness is considered to produce the thermal resistance R_{INT}. Figure 9 represents the measurements of film thickness. The results and the condition of numerical calculation are summarised in Table 3.

DISCUSSION

Figure 10 is obtained from the results of numerical calculation. The thermal resistance, R_{INT} determines both local heat flux and surface temperature of the solid flux film. Broken and solid curves are for Flux A and B respectively. Heat flux for Flux A is 4 % larger than one for Flux B at the same R_{INT}. Difference of solidus temperature and overall absorption coefficient is considered to be the reason though the contribution of radiation is relatively small comparing to the influence of R_{INT}. Flux A for example, the maximum local heat flux 3300 kWm^{-2} gives R_{INT} a value of $0.07x10^{-3}$ m^2KW^{-1}. This is approximately same value of thermal resistance for 5 μm thickness of air gap. The value 5 μm is equivalent to the average peak to peak roughness measurement for Flux A (Broken lines in the Fig. 10). $0.20x10^{-3}$ m^2KW^{-1} of R_{INT} is also obtained for Flux B. The value is equivalent to 12 μm of air gap and it is the same to the roughness of the flux film. Therefor the roughness of flux film is strongly effects to the value of $R_{INT.}$

Figure 11 shows the relationship between the solidus and the liquidus of the mold fluxes and maximum local heat flux in the commercial casting mold. (3CCM at Chiba Works, Kawasaki Steel Co.) The heat flux was measured by thermocouples on the centreline at just below meniscus of the mold. Relationship between the heat flux and the solidus shows better correlation than the liquidus. This means that the solidus controls the behaviour of thermal resistance at the interface of the mold and the flux film. The mold side interface temperature, T_p, can be determined with constant thermal conductivity, radiation properties and other boundary conditions by the numerical calculation. Figure 12 represents the relationship between the solidus and the $T_{p,}$ assuming the conditions of the calculation are as shown in Table 2 and 3. Fig. 12 shows good correspondence between T_p and (solidus – 360K). From the relationship, T_p is considered to be a maximum temperature to hold the roughness, which is equivalent to R_{INT}. It is

Watanabe et al. [4] and Tsutsumi et al. [6] have studied the formation of flux film roughness recently. However, the roughness of the film decreases when the initial value is large comparing with it solidus. Quenched glass samples for each fluxes A and B were annealed in a image furnace with LSM observation in order to examine the forming of roughness on the surface. The surfaces were smooth before annealing. After annealing at 1173K for 60 s, approximately 30 μm of rough surfaces appeared

on both samples. Therefor solidus determines the value of R_{INT} when the mold flux tends to form crystalline phase.

CONCLUSIONS

Basic type mold fluxes were investigated to clarify the mechanism of determining heat flux at the meniscus region in the mold. The results of measuring heat transfer properties, numerical calculations and casting experiments are summarised as follows. The solidus of mold fluxes mainly effect roughness of flux film surface obtained from casting mold and determines local heat flux. It is the main reason of reduction of heat flux using high-melting-point mold flux that the roughness increases with the solidus of mold flux.

ACKNOWLEDGEMENTS

The authors are thankful to Professor Seetharaman, co-chairman of Department of Material Science and Engineering for giving us a chance to present the study of mold flux.

REFERENCE

[1] T. Chikano, K. Ichikawa and O. Nomura: Shinagawa Technical Report, 31(1988), 75

[2] A. Yamauchi, K. Sorimachi, T. Sakuraya and T. Fujii: ISIJ International 33 (1993) 1, 140

[3] J. Cho, H. Shibata, T. Emi and M. Suzuki: ISIJ Int. 38(1998), 5, 440

[4] Watanabe et al. NKK Gihou No.157 (1997) 3, 1

[5] K. C. Mills: 3rd Int. Conf. on Molten Slag and Fluxes, 1988,p.229 Glasgow, The Institute of Metals.

[6] Tsutsumi et al.: ISIJ International 39 (1999) 11, p1150

[7] H. Alan Fine, T. Engh and J. Elliott: Metall. Trans., 7B (1976), 277

List of symbols

a: absorption coefficient	m^{-1}
d: thickness	m
h: heat transfer coefficient	$Wm^{-2}K^{-1}$
n: refraction index	-
q: heat flux	Wm^{-2}
R: thermal resistance	m^2KW^{-1}
T: temperature	K
α: radiation heat transfer coefficient	$Wm^{-2}K^{-1}$
ε: emissivity	-
λ: thermal conductivity of mold flux	$Wm^{-1}K^{-1}$
σ: Stefan-Bolzmann constant	$=5.669x10^{-11}$ $kWm^{-2}K^{-4}$

Subscription:
c: coduction heat transfer
INT: interface between mold and solid flux
l: liquid phase of mold flux
m: sueface of mold
p: mold flux or surface of mold flux
r: radiation heat transfer
s: surface of solidifying shell or AlN plate

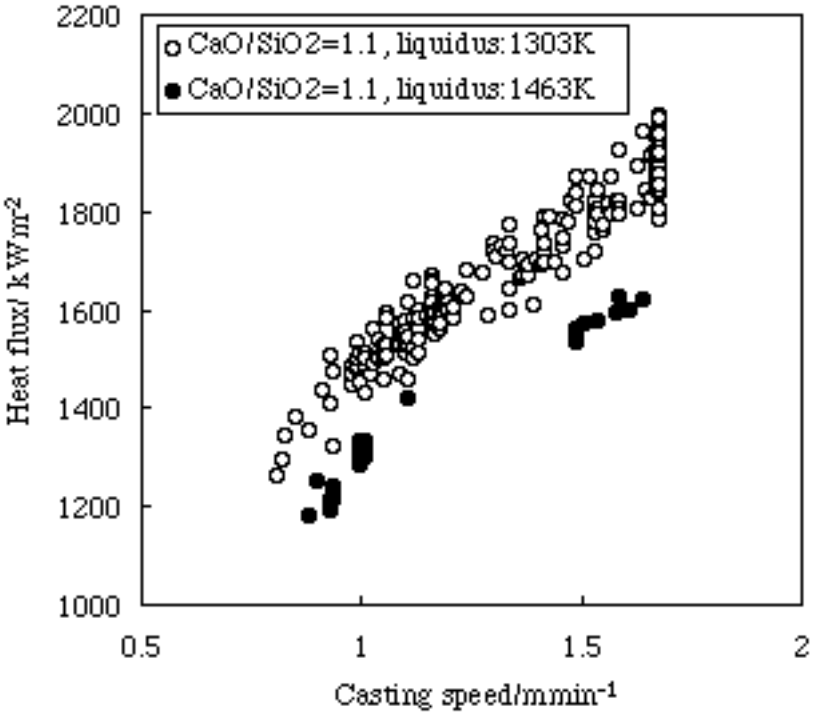

Fig.1 Aveage heat flux measured by temperature difference between inlet and outlet cooling water and the flow rate in the commercial casting mold at Chiba 3CCM. (0.00025%C-ULC steel)

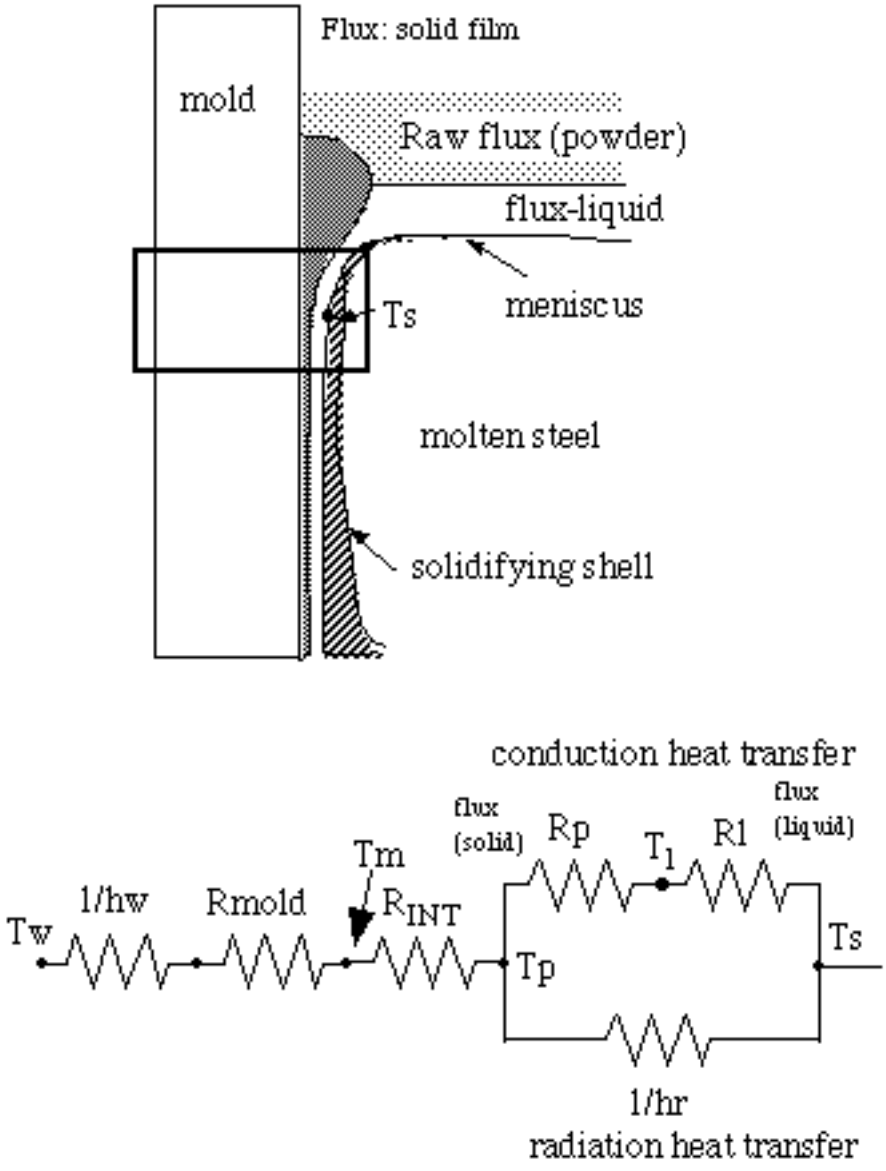

Fig.2 Heat transfer model at steady state in the mold

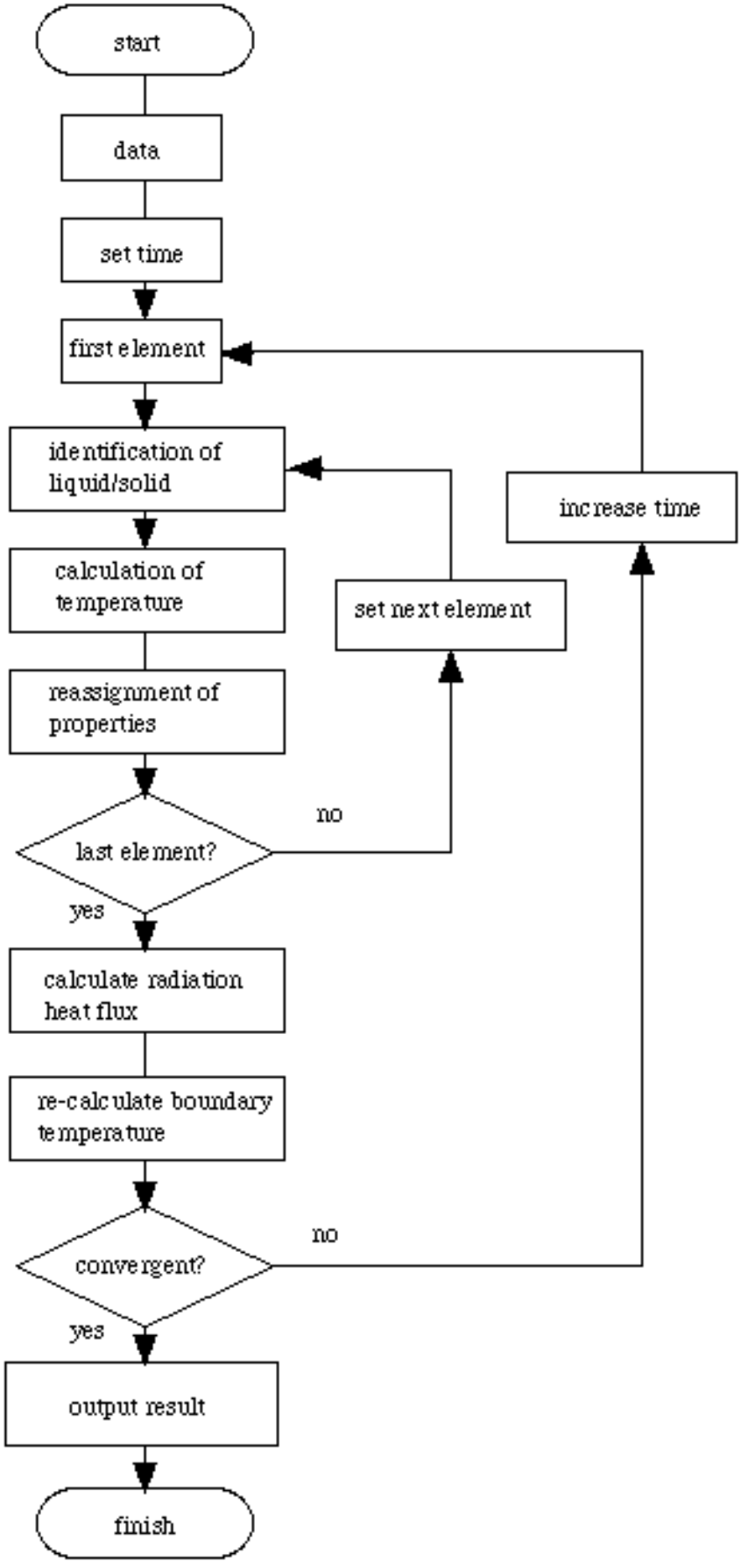

Fig. 3 Simplified flow diagram of numerical calculation program

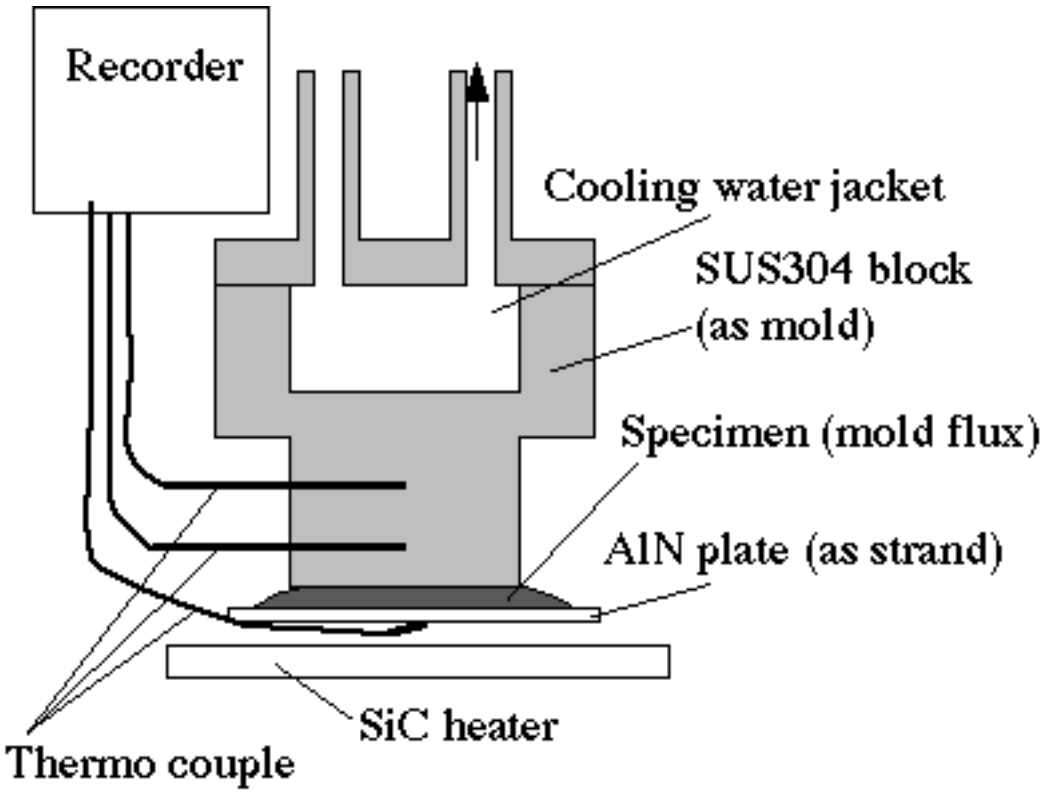

Fig. 4 Schematic representation of apparatus for measuring heat transfer properties of mold flux

Ts=1470～1590K
Tm=500～1000K

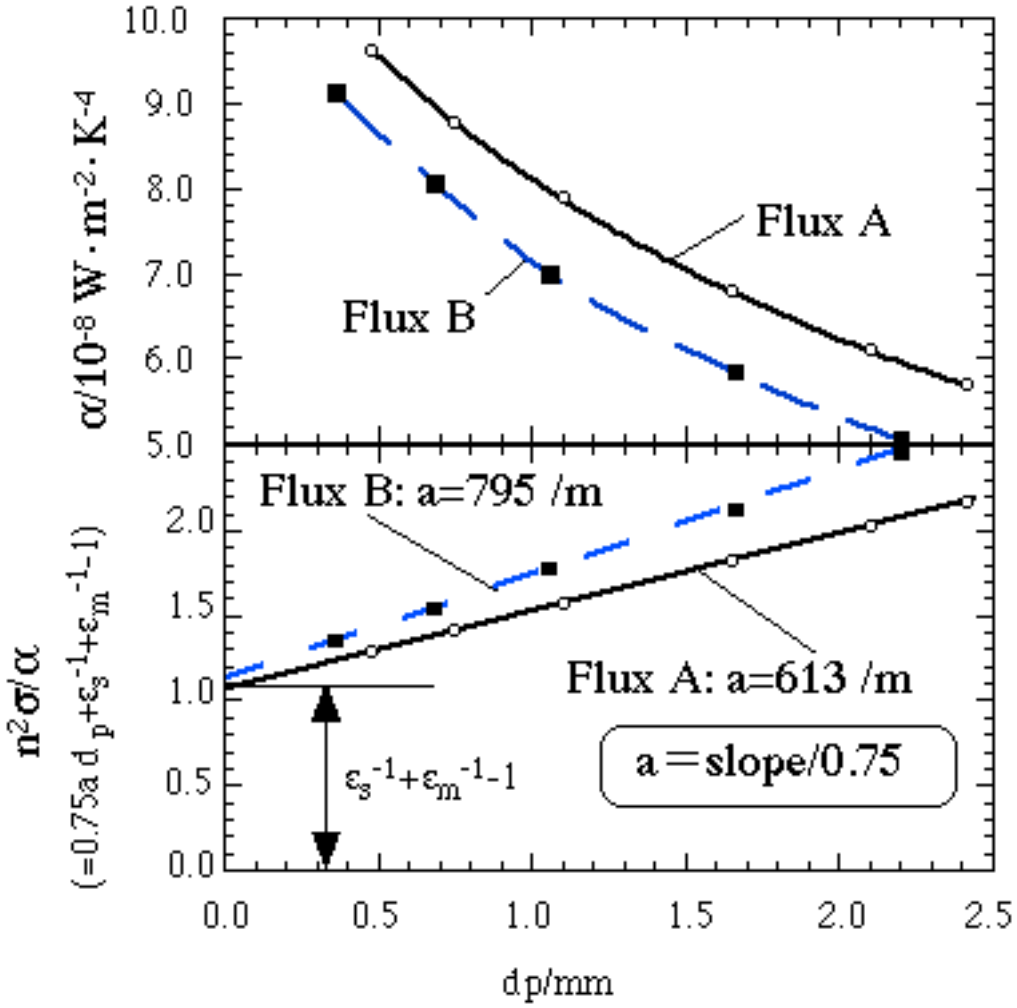

Fig. 5 An exapmle of parallel plate method result

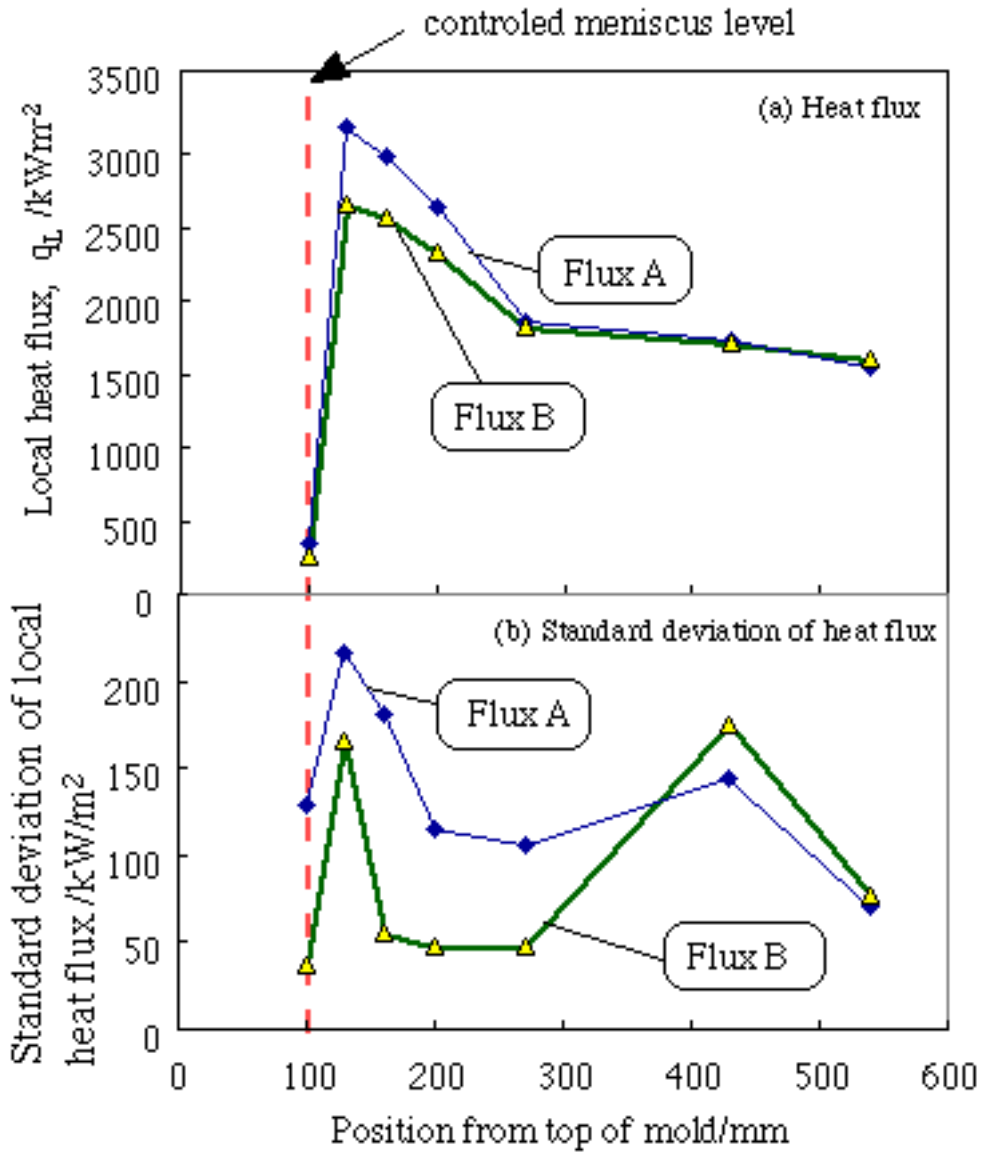

Fig. 6 Local heat flux and standard deviation of the heat flux.

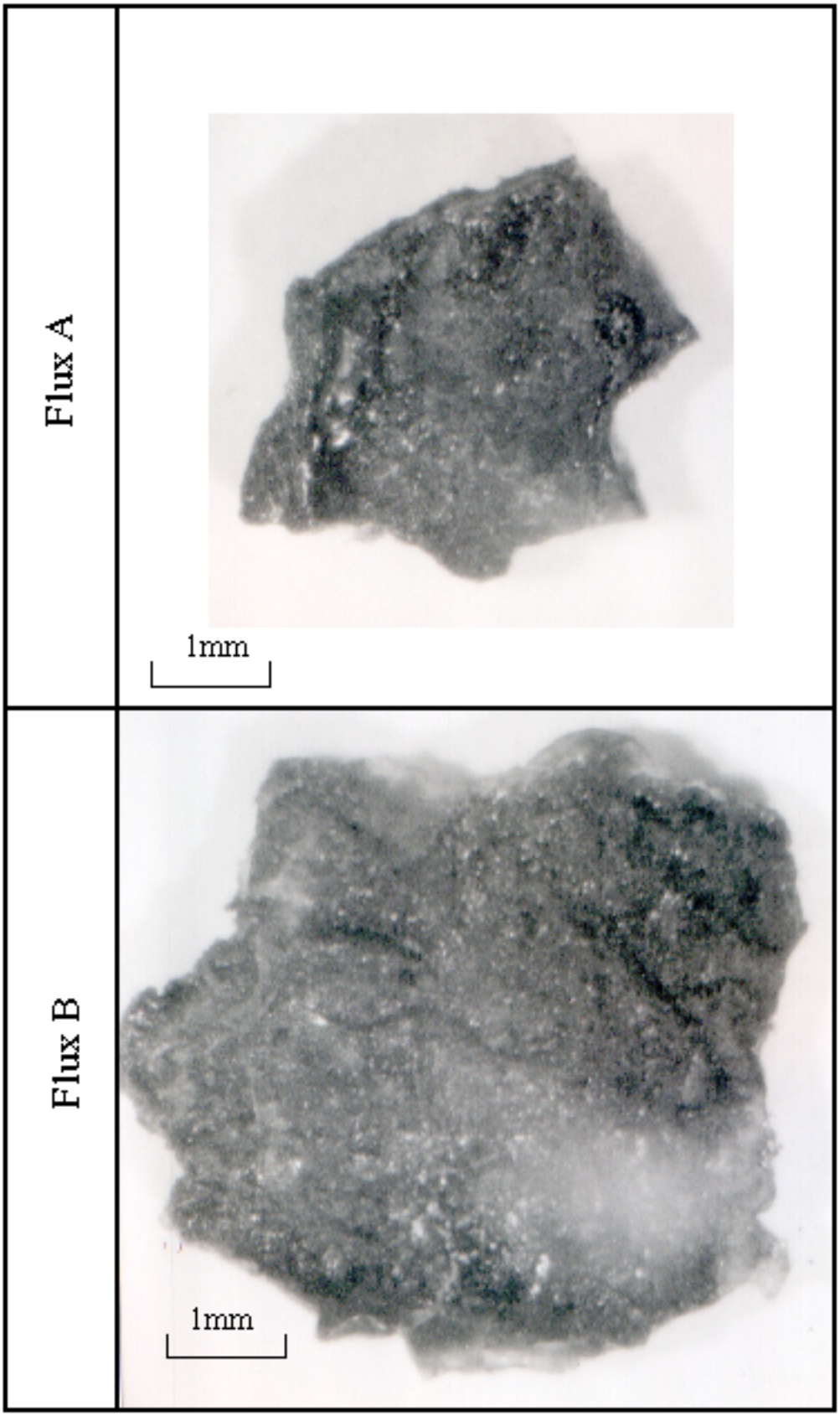

Fig. 7 Out looking of flux film pieces obtained from continuous casting machine (Pilot plant)

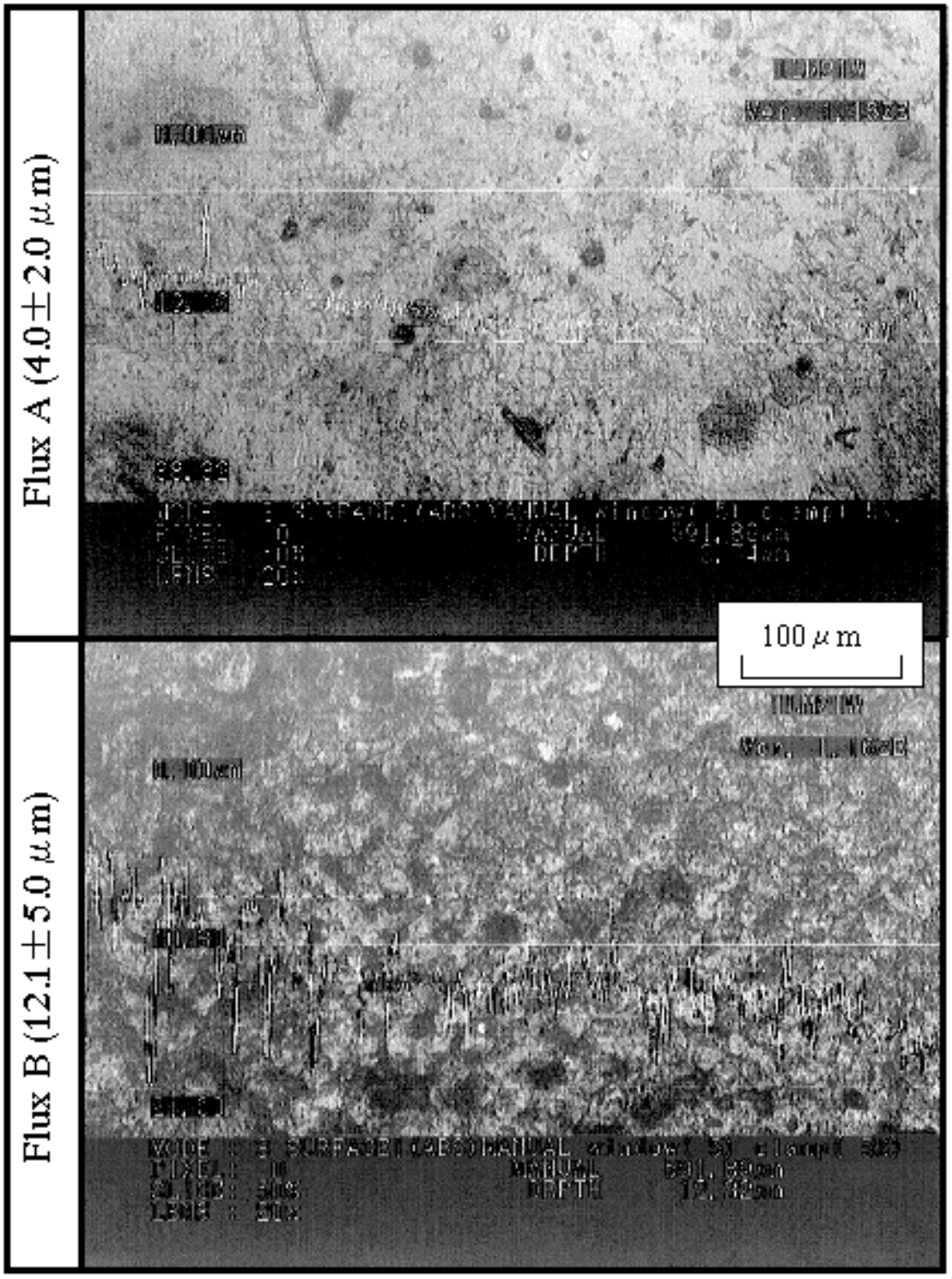

Fig.8 Laser Scanning Microscopic images of the flux film surface

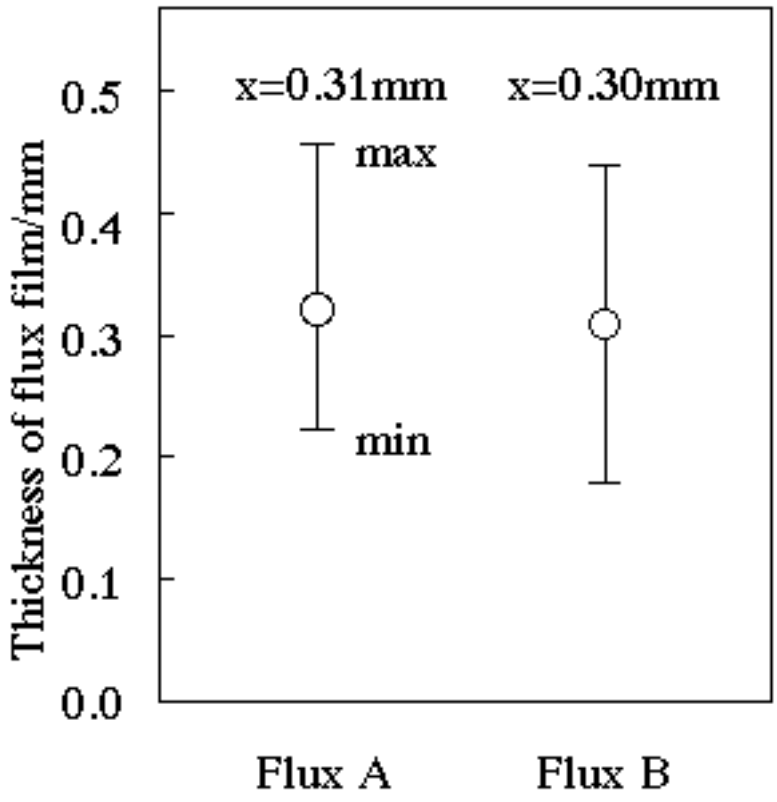

Casting speed: 1.60 m/min (26.7mm/s)
Frequency of mold osillation: 112 cpm (1.87Hz)
Stroke of mold oscillation: ±3.9 mm

Fig. 9 Thickness of flux film obtained below mold

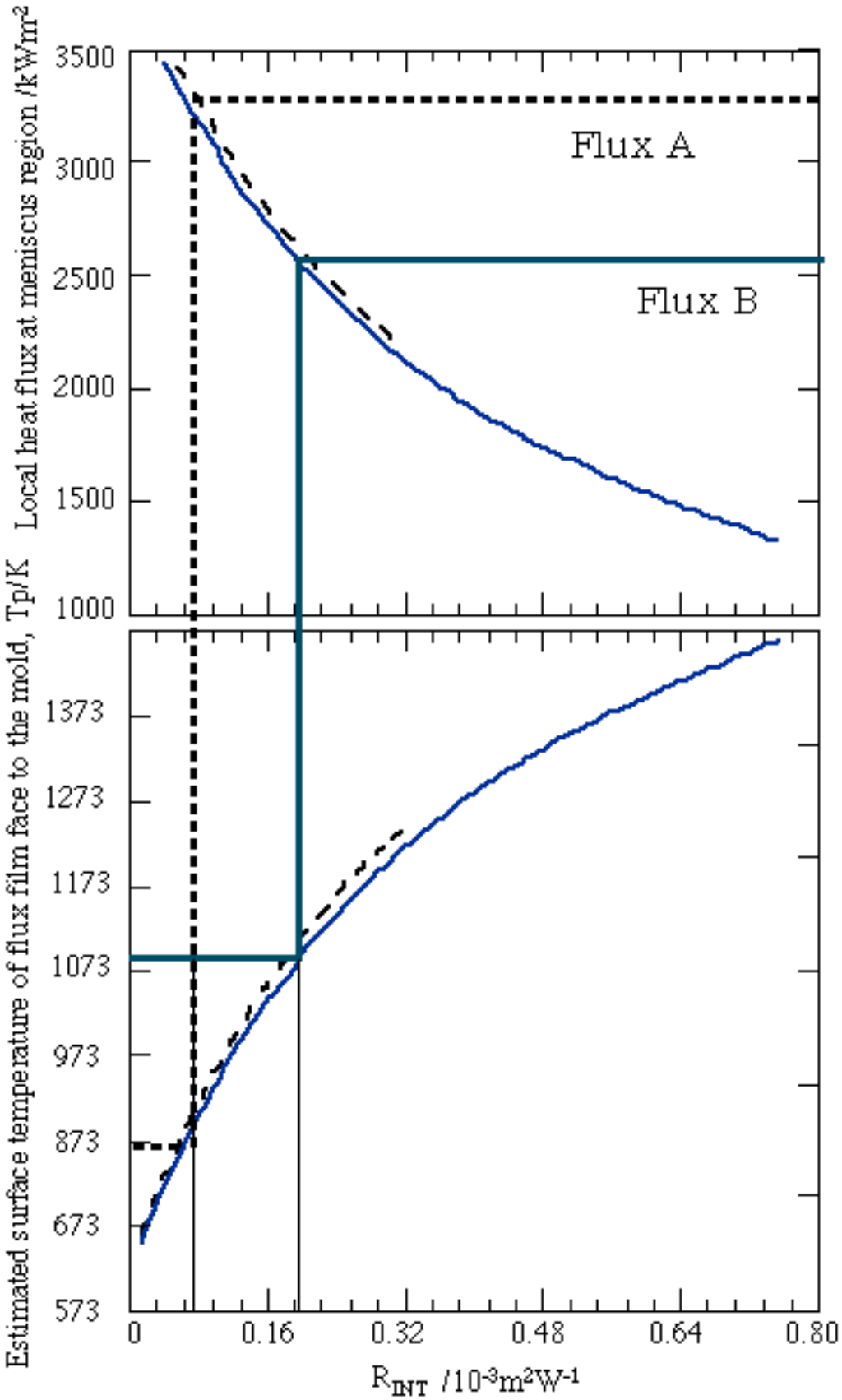

Fig. 10 Relationship between R_{INT}, T_P and local heat flux derived from numerical simulation at meniscus region.

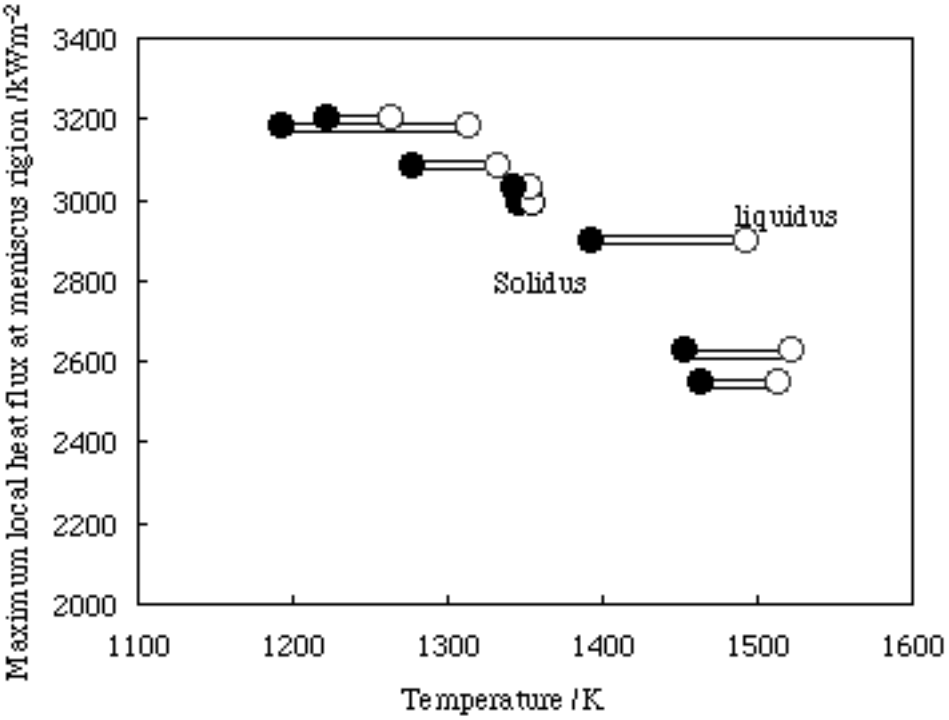

Fig. 11 Relationship between measured solidus, liquidus of mold flux and maximum local heat flux at meniscus region in commercial casting of Chiba 3CCM, Kawasaki Steel Co. (Casting speed: 1.6mpm)

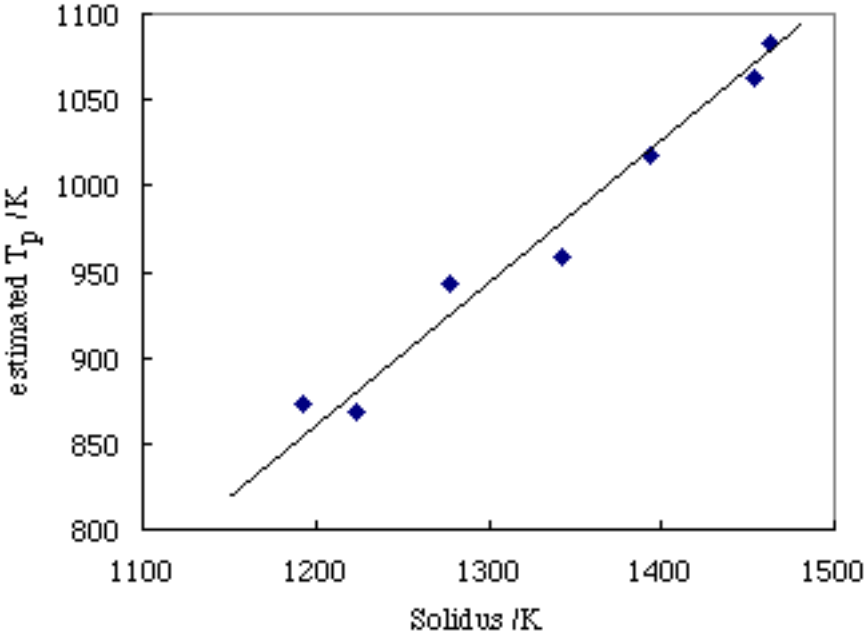

Fig. 12 Relationship between solidus and estimated T_p with the relationship shown in Fig. 10

Table 1 Chemical composition (wt%) of mold flux

Flux	A	B
SiO_2	28.5	31.3
Al_2O_3	5.3	2.1
CaO	26.9	40.1
Fe_2O_3	2.4	0.2
Na_2O	15.0	8.0
MgO	6.3	0.1
F	8.5	11.4
Li_2O		3.9
CaO/SiO_2	0.95	1.28
solidus[K]	1223	1463
liquidus[K]	1263	1513

Table 2 Heat transfer properties of mold flux

Property		Flux A	Flux B
λ_C [$Wm^{-1}K^{-1}$]	crystalline	1.07	1.14
	glassy	0.86	0.89
$\varepsilon_s^{-1}+\varepsilon_m^{-1}-1$		1.1	
a [m^{-1}]		613	795

reference[3]
crystalline: 5000～15000m^{-1}
glass,liquid: 250～700m^{-1}

Table 3 Condition of numerical calculation

Total thickness of flux film dp[mm]	0.31
Thermal resistance of mold, Rm [m^2K/kW]	0.076
$1/h_w$ [m^2K/kW]	0.035
Temperature of cooling water [°C]	40 (313 K)
Surface temperature of steel shell at meniscus [°C]	1520 (1793K)